Supplementary Information for

Coseismic Coulomb Stress Changes on Intraplate Faults in the Western Quebec Seismic Zone, Canada: Implications for Seismic Hazards

Jeremy M. Rimando[1], Alexander L. Peace[1], Katsuichiro Goda[2], Navid Sirous[2], Philippe Rosset[3], Luc Chouinard[3]

[1]School of Earth, Environment & Society, McMaster University, 1280 Main Street W., Hamilton, ON, L8S 4K1, Canada

[2]Department of Earth Sciences, Western University, 1151 Richmond Street N., London, ON, N6A 5B7, Canada

[3]Department of Civil Engineering, McGill University, 817 Sherbrooke St W., Montreal, QC H3A 0C3, Canada

Contents of this file

Figures S1 to S20

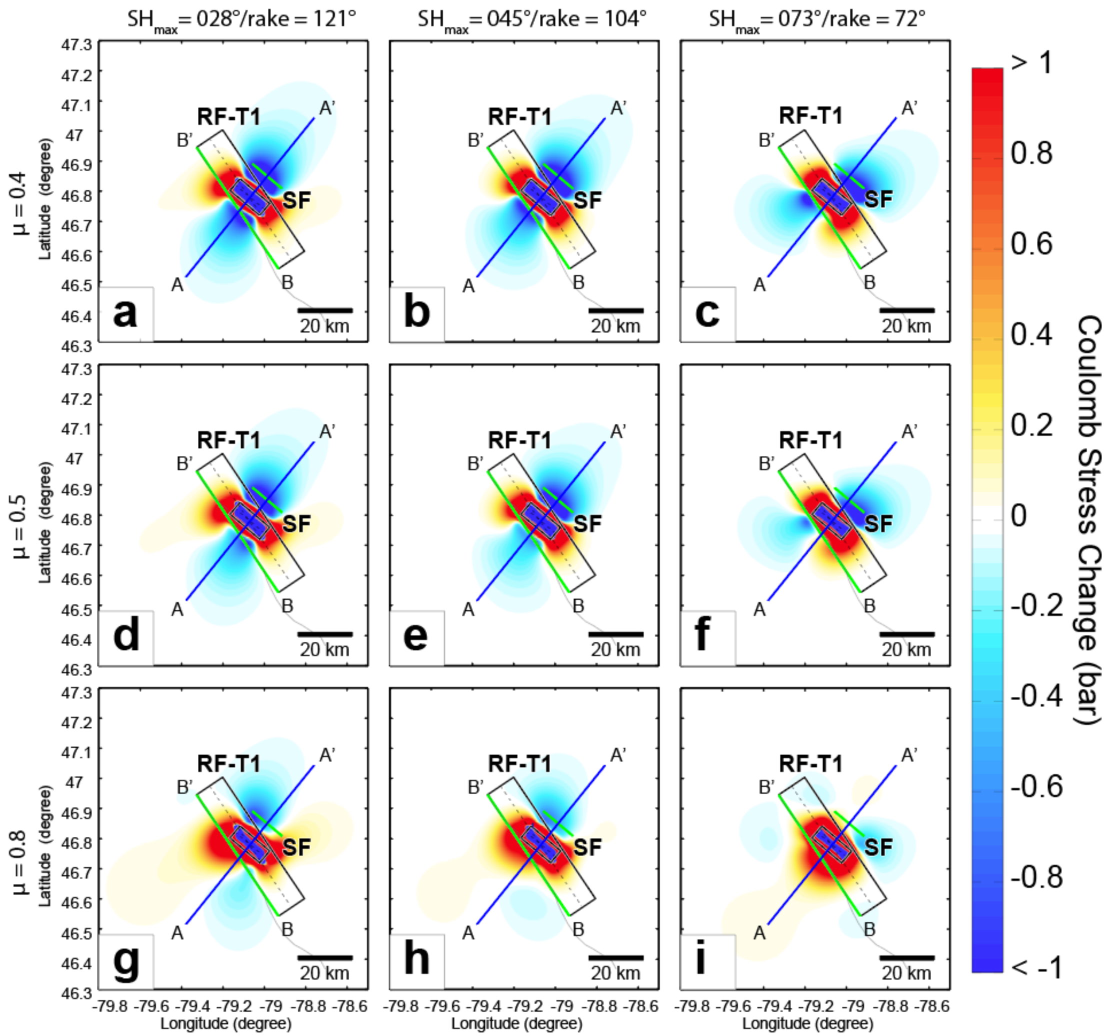

Figure S1. 1935 *Mw* 6.1 Temiscaming Earthquake nodal plane 1 Coulomb stress change maps. Coulomb stress changes for the SW-dipping source fault plane (strike = 130°, dip = 45°, rake = 80°), as seen in map view (10-km-depth slice). The sensitivity of stress change distributions was tested using the following receiver fault rake values (or maximum horizontal stress azimuths) as follows: (**a, d, g**) 121° (or S_{Hmax} = 028°), (**b, e, h**) 104° (or SH_{max} = 045°), and (**c, f, i**) 72° (or SH_{max} = 073°); and coefficient of friction) values as follows: (**a, b, c**) μ = 0.4, (**b, e, h**) μ = 0.5, and (**c, f, i**) μ = 0.8.

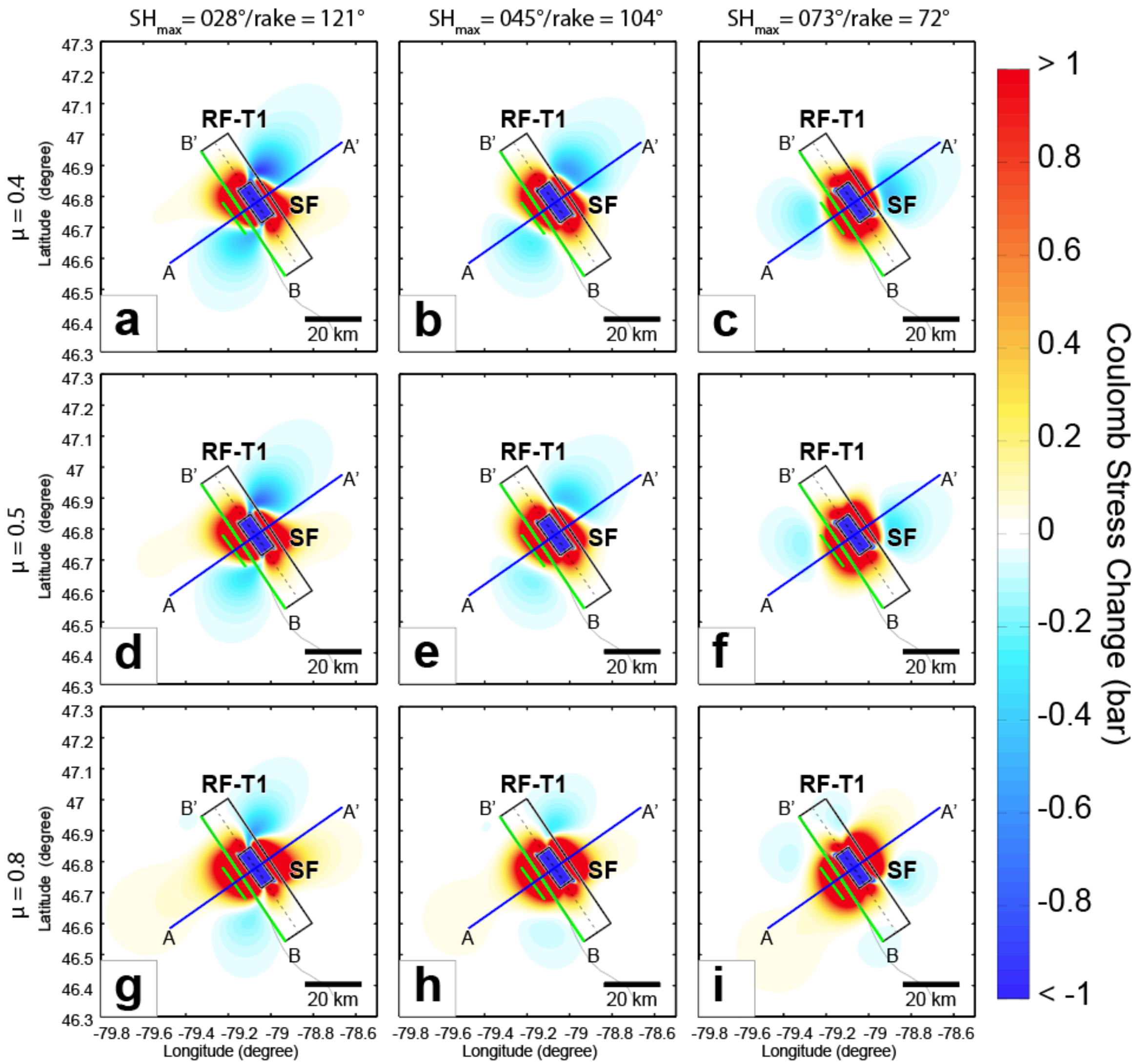

Figure S2. 1935 *M*$_W$ 6.1 Temiscaming Earthquake nodal plane 2 Coulomb stress change maps. Coulomb stress changes for the NE-dipping source fault plane (strike = 324°, dip = 46°, rake = 100°), as seen in map view (10-km-depth slice). The sensitivity of stress change distributions was tested using the following receiver fault rake values (or maximum horizontal stress azimuths) as follows: (**a, d, g**) 121° (or S_{Hmax} = 028°), (**b, e, h**) 104° (or SH_{max} = 045°), and (**c, f, i**) 72° (or SH_{max} = 073°); and coefficient of friction) values as follows: (**a, b, c**) μ = 0.4, (**b, e, h**) μ = 0.5, and (**c, f, i**) μ = 0.8.

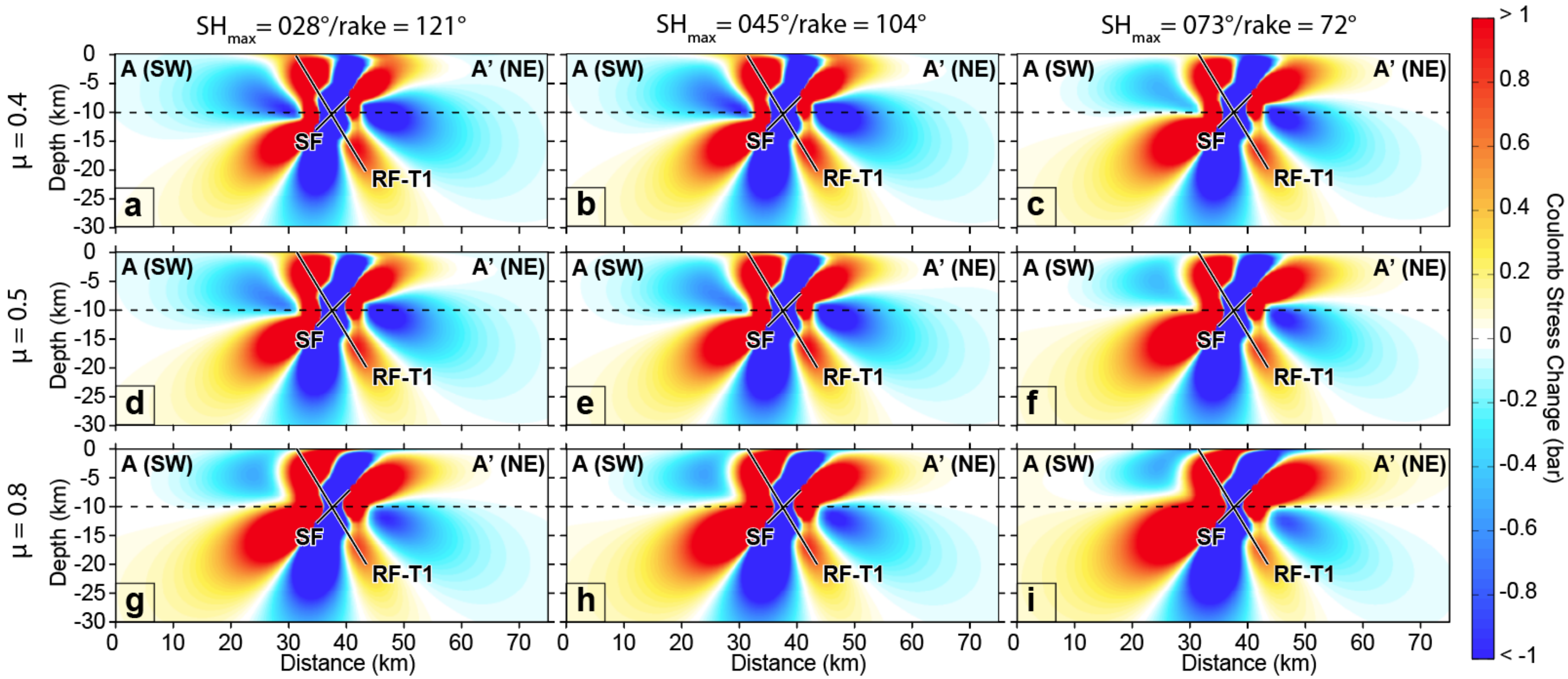

Figure S3. 1935 *Mw* 6.1 Temiscaming Earthquake nodal plane 1 Coulomb stress change cross-sections. Coulomb stress changes for the SW-dipping source fault plane (strike = 130°, dip = 45°, rake = 80°), as seen in cross-sectional view. The sensitivity of stress change distributions was tested using the following receiver fault rake values (or maximum horizontal stress azimuths) as follows: (**a, d, g**) 121° (or S_{Hmax} = 028°), (**b, e, h**) 104° (or SH_{max} = 045°), and (**c, f, i**) 72° (or SH_{max} = 073°); and coefficient of friction) values as follows: (**a, b, c**) μ = 0.4, (**b, e, h**) μ = 0.5, and (**c, f, i**) μ = 0.8

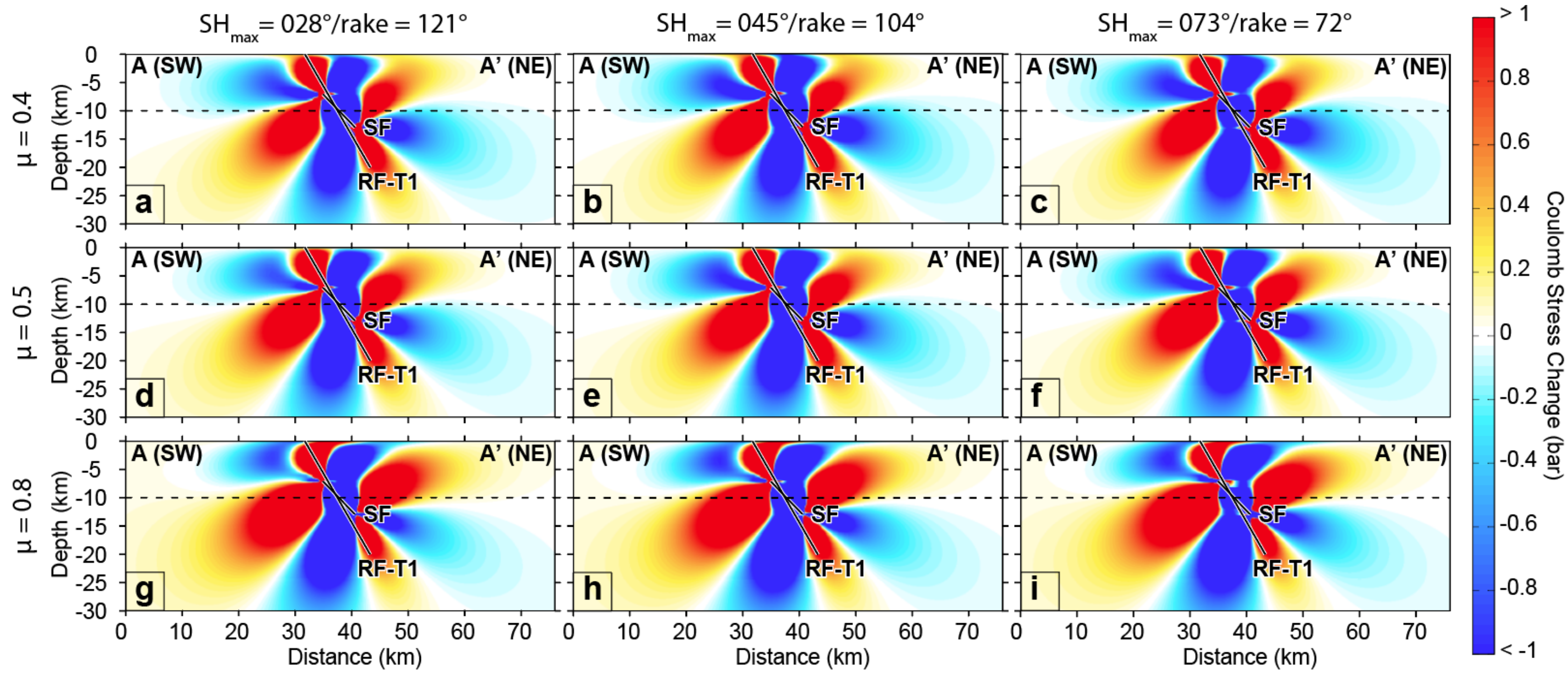

Figure S4. 1935 *Mw* 6.1 Temiscaming Earthquake nodal plane 2 Coulomb stress change cross-sections. Coulomb stress changes for the NE-dipping source fault plane (strike = 324°, dip = 46°, rake = 100°), as seen in cross-sectional view. The sensitivity of stress change distributions was tested using the following receiver fault rake values (or maximum horizontal stress azimuths) as follows: (**a, d, g**) 121° (or S_{Hmax} = 028°), (**b, e, h**) 104° (or SH_{max} = 045°), and (**c, f, i**) 72° (or SH_{max} = 073°); and coefficient of friction) values as follows: (**a, b, c**) μ = 0.4, (**b, e, h**) μ = 0.5, and (**c, f, i**) μ = 0.8.

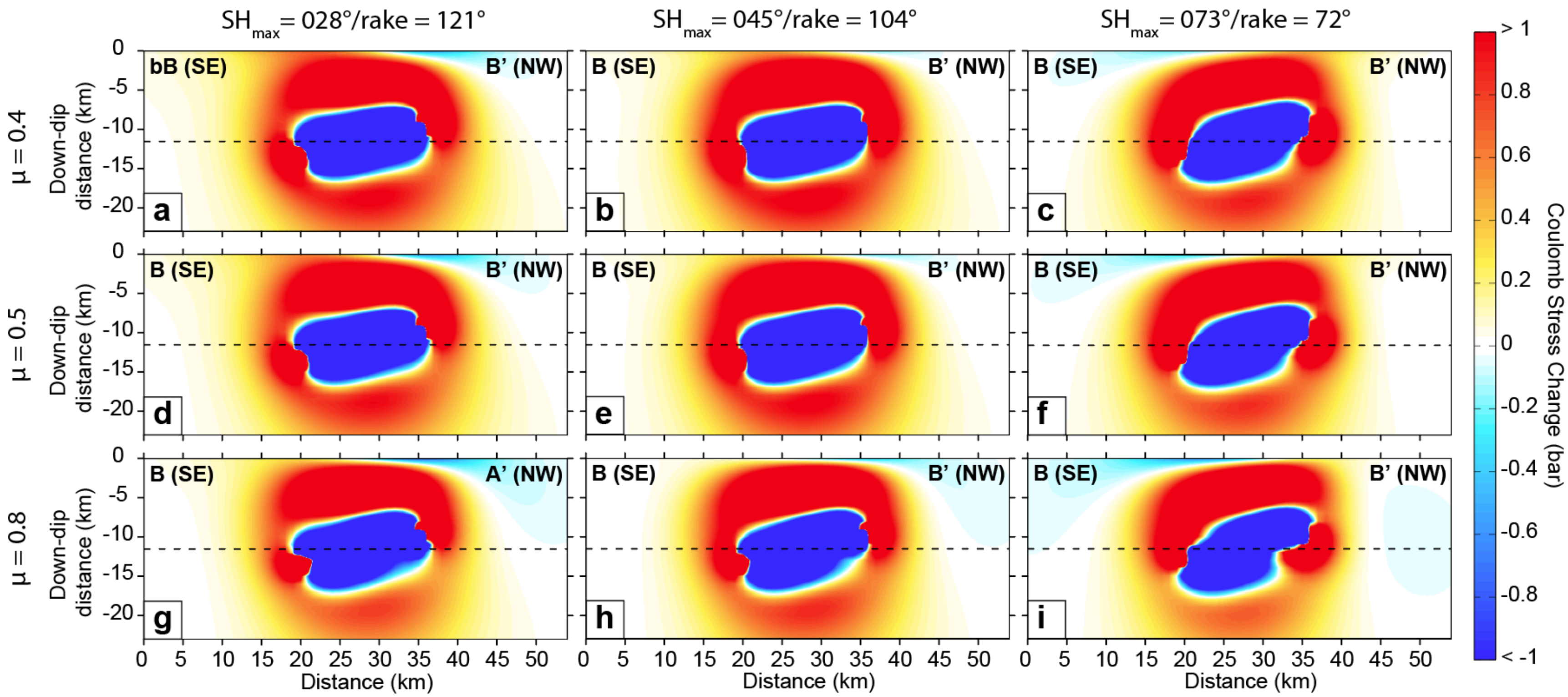

Figure S5. 1935 *Mw* 6.1 Temiscaming Earthquake nodal plane 1 Coulomb stress change on receiver faults. Coulomb stress changes for the SW-dipping source fault plane (strike = 130°, dip = 45°, rake = 80°), as seen on the receiver fault plane. The sensitivity of stress change distributions was tested using the following receiver fault rake values (or maximum horizontal stress azimuths) as follows: (**a, d, g**) 121° (or S_{Hmax} = 028°), (**b, e, h**) 104° (or SH_{max} = 045°), and (**c, f, i**) 72° (or SH_{max} = 073°); and coefficient of friction) values as follows: (**a, b, c**) μ = 0.4, (**b, e, h**) μ = 0.5, and (**c, f, i**) μ = 0.8.

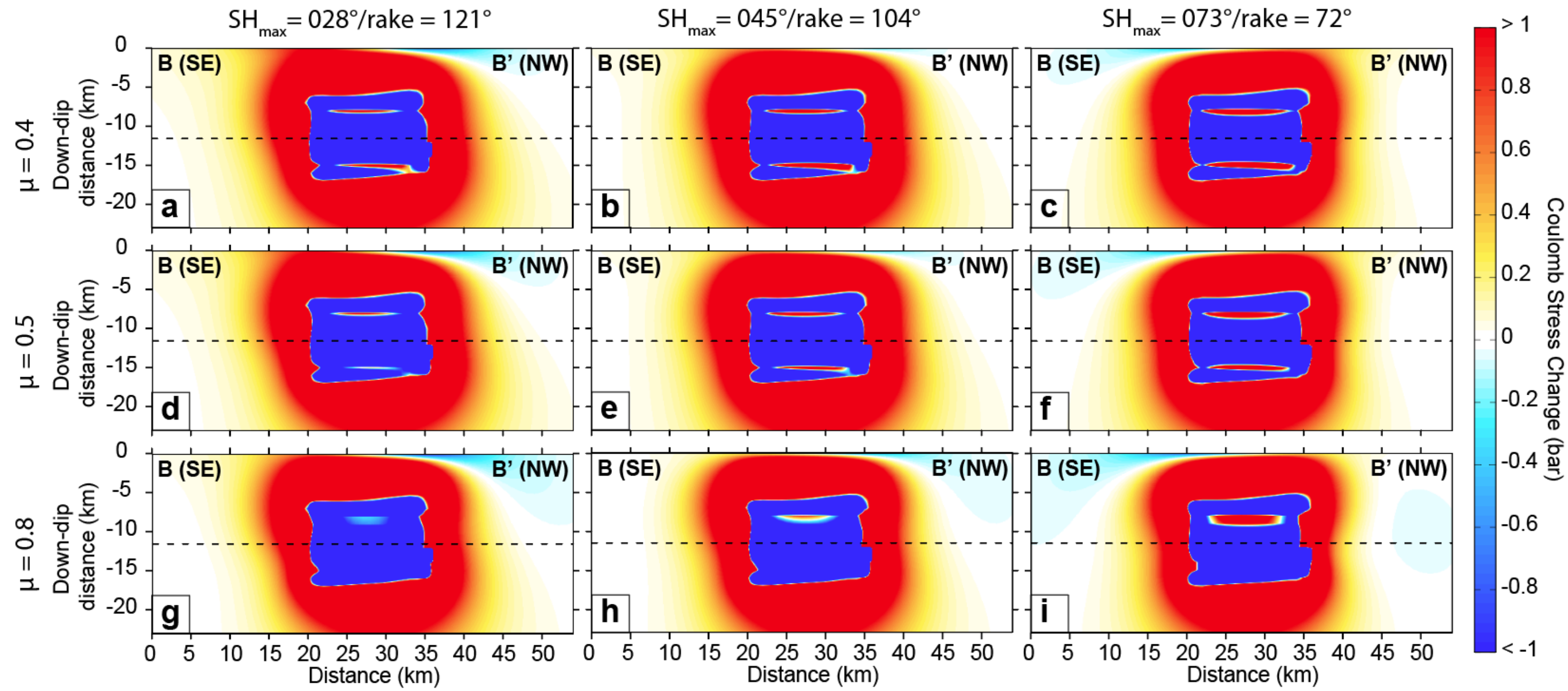

Figure S6. 1935 *Mw* 6.1 Temiscaming Earthquake nodal plane 2 Coulomb stress change on receiver faults. Coulomb stress changes for the NE-dipping source fault plane (strike = 324°, dip = 46°, rake = 100°), as seen on the receiver fault plane. The sensitivity of stress change distributions was tested using the following receiver fault rake values (or maximum horizontal stress azimuths) as follows: (**a, d, g**) 121° (or S_{Hmax} = 028°), (**b, e, h**) 104° (or SH_{max} = 045°), and (**c, f, i**) 72° (or SH_{max} = 073°); and coefficient of friction) values as follows: (**a, b, c**) μ = 0.4, (**b, e, h**) μ = 0.5, and (**c, f, i**) μ = 0.8.

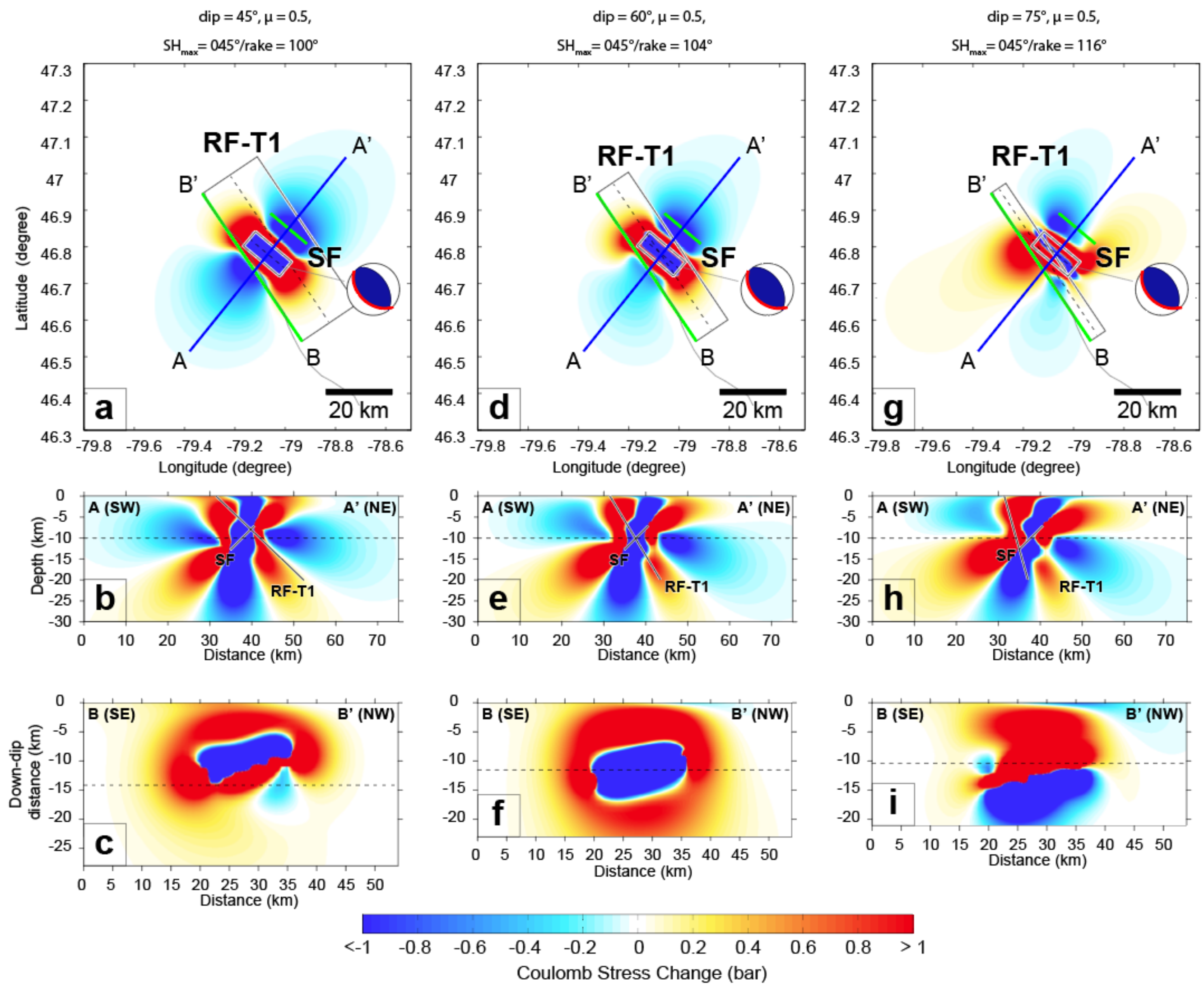

Figure S7. 1935 *Mw* 6.1 Temiscaming Earthquake nodal plane 1 receiver fault dip sensitivity test. Coulomb stress changes for the SW-dipping source fault plane (strike = 130, dip = 45, rake = 80), as seen in map view at 10-km-depth (a, d, g), in cross-section (b, e, h), and as projected on the receiver fault plane (c, f, i). The sensitivity of stress change distributions to receiver fault plane dip was tested using the following values: 45 ° (a, b, c), 60 ° (d, e, f), and 75 ° (r, h, i). All calculations assumed a coefficient of friction (μ) of 0.5 and a receiver fault plane rake based on a maximum horizontal stress value of 45°.

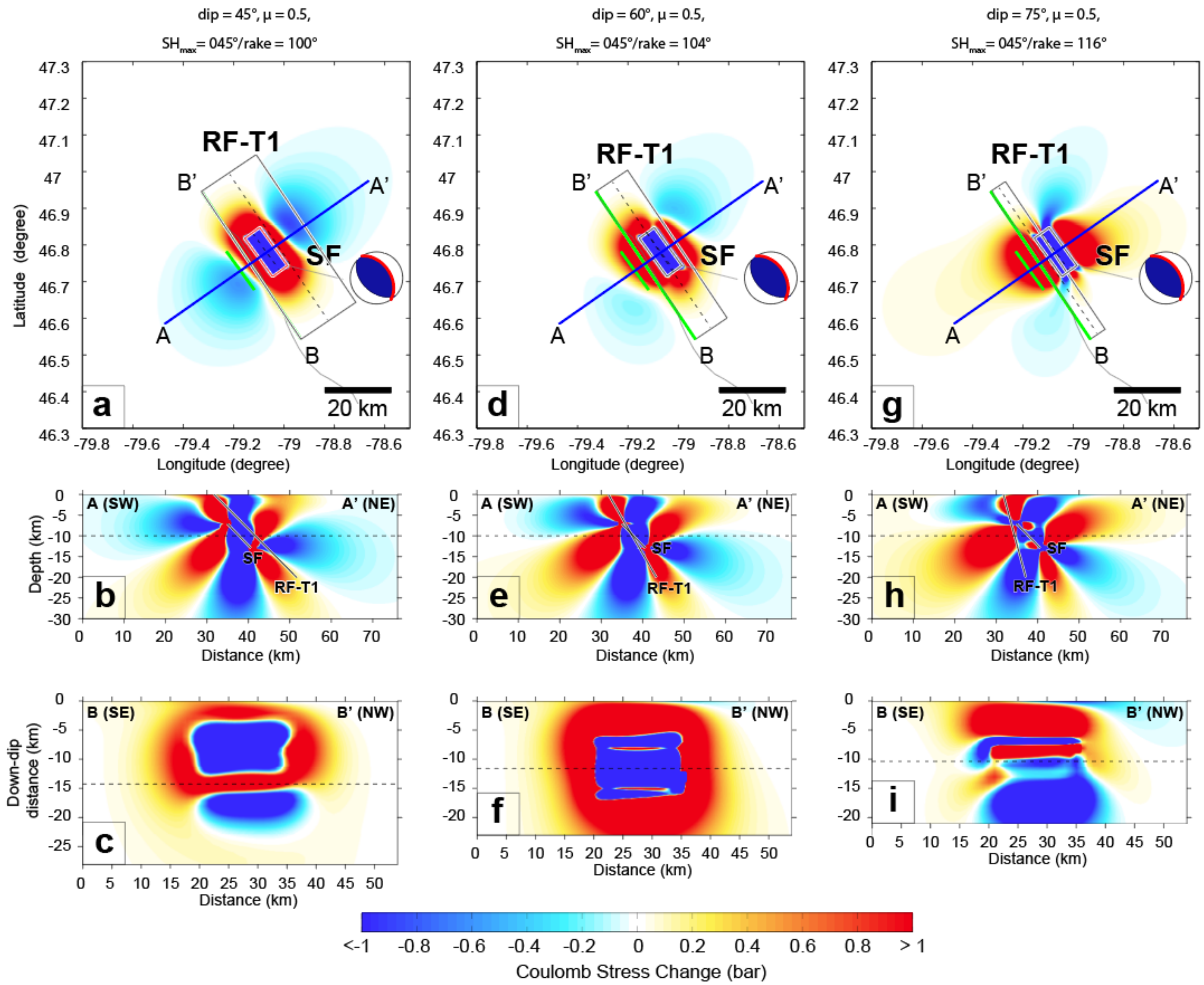

Figure S8. 1935 *M*$_W$ 6.1 Temiscaming Earthquake nodal plane 2 receiver fault dip sensitivity test. Coulomb stress changes for the NE-dipping source fault plane (strike = 324, dip = 46, rake = 100), as seen in map view at 10-km-depth (**a, d, g**), in cross-section (**b, e, h**), and as projected on the receiver fault plane (**c, f, i**). The sensitivity of stress change distributions to receiver fault plane dip was tested using the following values: 45 ° (**a, b, c**), 60 ° (**d, e, f**), and 75 ° (**r, h, i**). All calculations assumed a coefficient of friction (μ) of 0.5 and a receiver fault plane rake based on a maximum horizontal stress value of 45°.

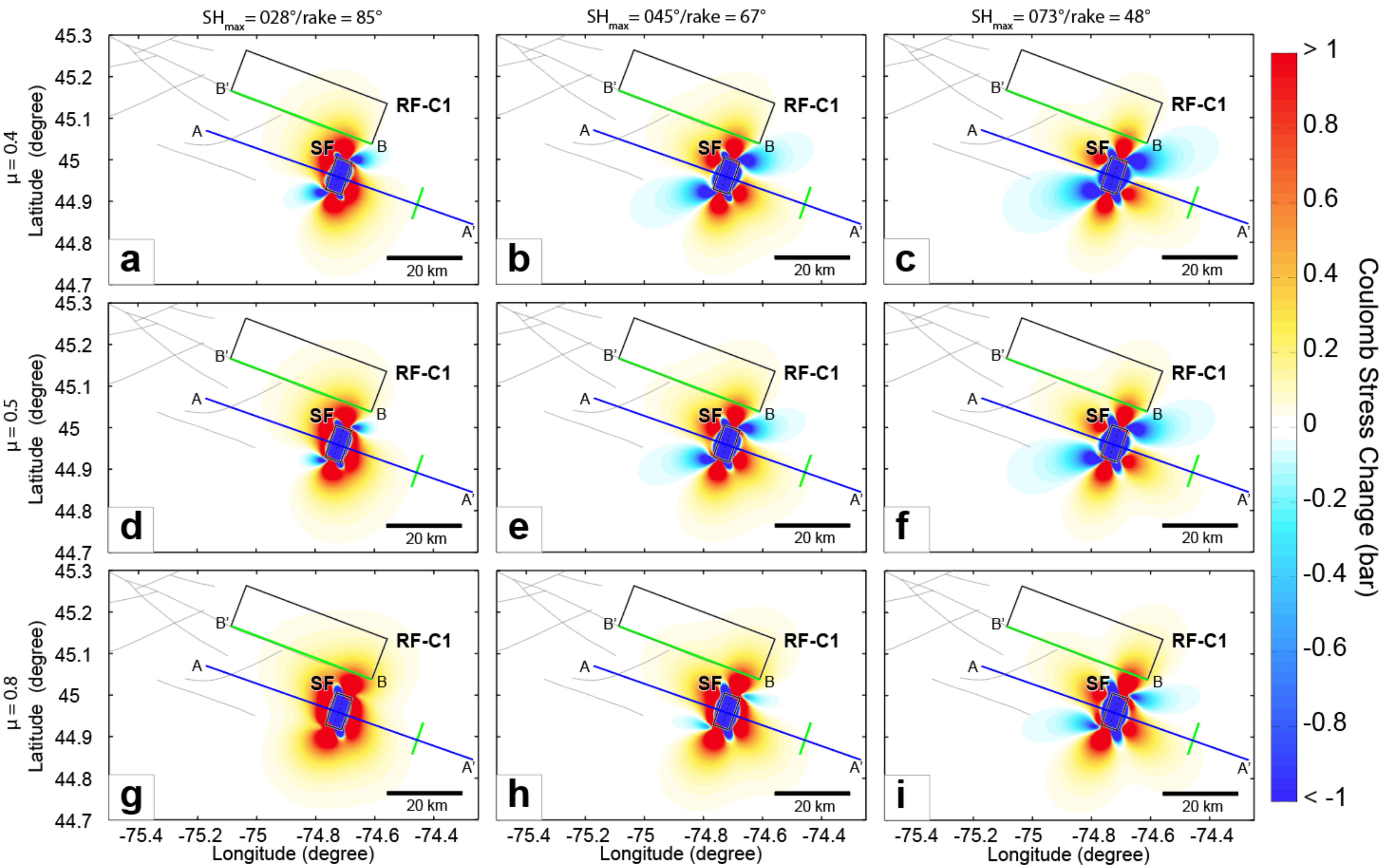

Figure S9. 1944 *Mw* 5.8 Cornwall-Massena Earthquake nodal plane 1 Coulomb stress change maps. Coulomb stress changes for the NW-dipping source fault plane (strike = 199°, dip = 42°, rake = 149°), as seen in map view (20-km-depth slice). The sensitivity of stress change distributions was tested using the following receiver fault rake values (or maximum horizontal stress azimuths) as follows: (**a, d, g**) 85° (or S_{Hmax} = 028°), (**b, e, h**) 67° (or SH_{max} = 045°), and (**c, f, i**) 48° (or SH_{max} = 073°); and coefficient of friction) values as follows: (**a, b, c**) μ = 0.4, (**b, e, h**) μ = 0.5, and (**c, f, i**) μ = 0.8.

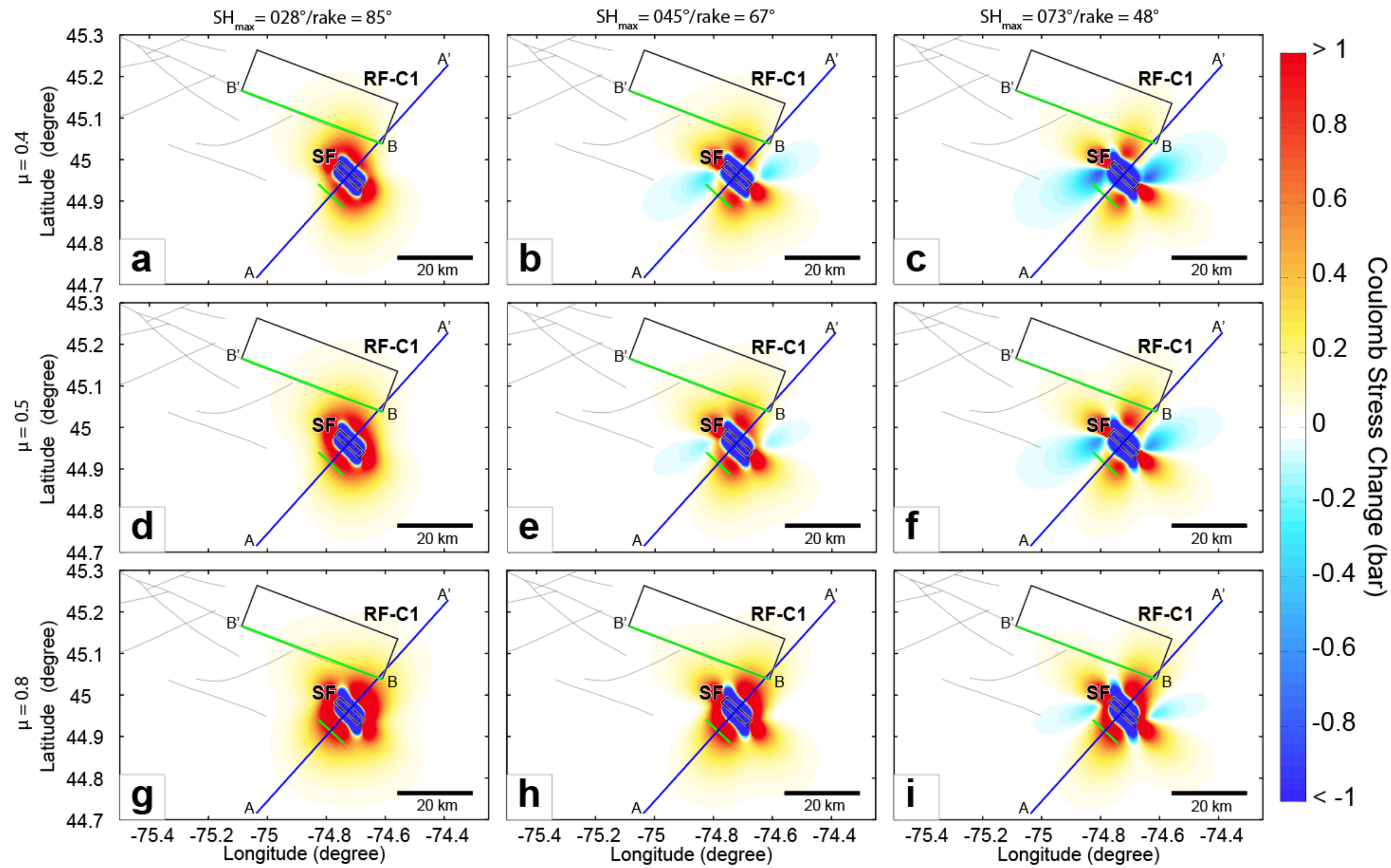

Figure S10. 1944 *M*$_W$ 5.8 Cornwall-Massena Earthquake nodal plane 2 Coulomb stress change maps. Coulomb stress changes for the NE-dipping source fault plane (strike = 313°, dip = 70°, rake = 52°), as seen in map view (20-km-depth slice). The sensitivity of stress change distributions was tested using the following receiver fault rake values (or maximum horizontal stress azimuths) as follows: (**a, d, g**) 85° (or S_{Hmax} = 028°), (**b, e, h**) 67° or SH_{max} = 045°, and (**c, f, i**) 48° (or SH_{max} = 073°); and coefficient of friction) values as follows: (**a, b, c**) μ = 0.4, (**b, e, h**) μ = 0.5, and (**c, f, i**) μ = 0.8.

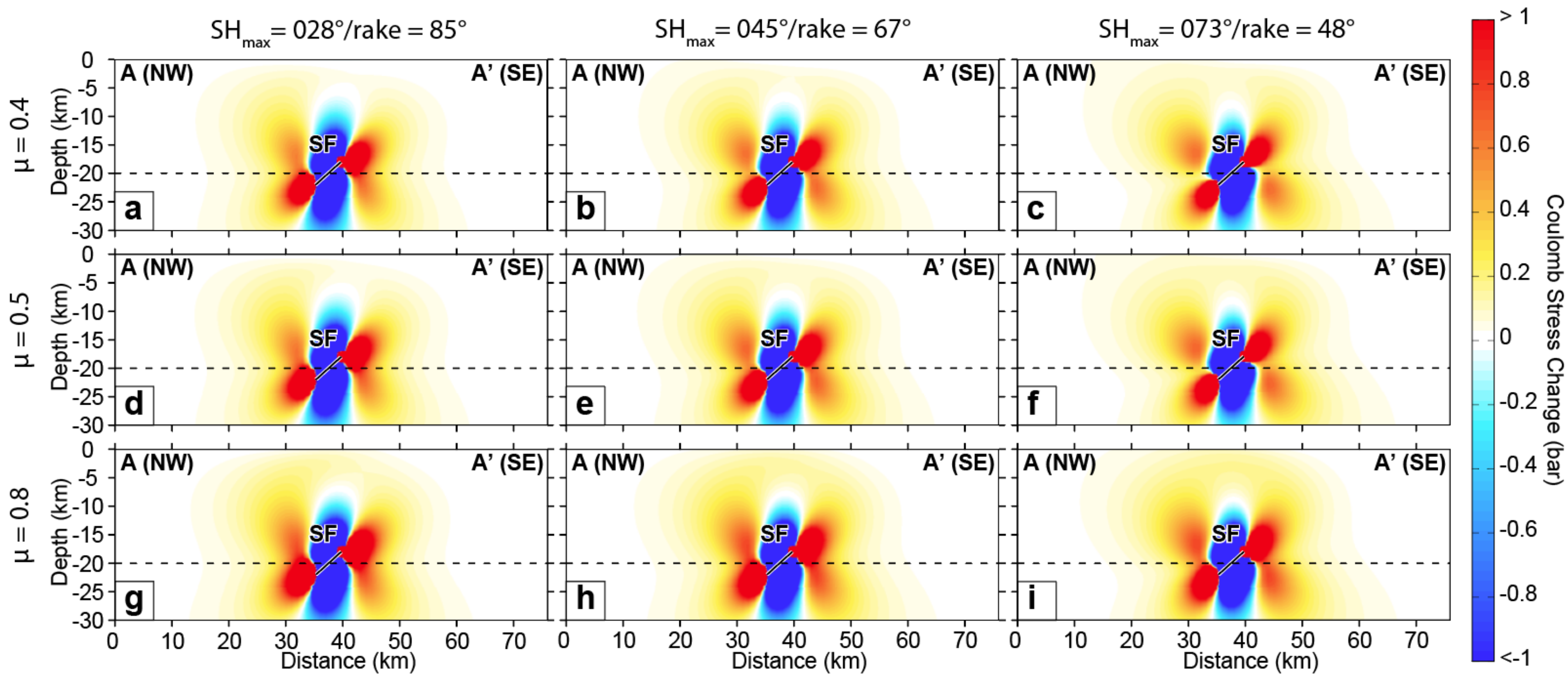

Figure S11. 1944 *M*$_W$ 5.8 Cornwall-Massena Earthquake nodal plane 1 Coulomb stress change cross-sections. Coulomb stress changes for the NW-dipping source fault plane (strike = 199°, dip = 42°, rake = 149°), as seen in cross-sectional view. The sensitivity of stress change distributions was tested using the following receiver fault rake values (or maximum horizontal stress azimuths) as follows: (**a, d, g**) 85° (or S$_{Hmax}$ = 028°), (**b, e, h**) 67° (or SH$_{max}$ = 045°), and (**c, f, i**) 48° (or SH$_{max}$ = 073°); and coefficient of friction) values as follows: (**a, b, c**) μ = 0.4, (**b, e, h**) μ = 0.5, and (**c, f, i**) μ = 0.8.

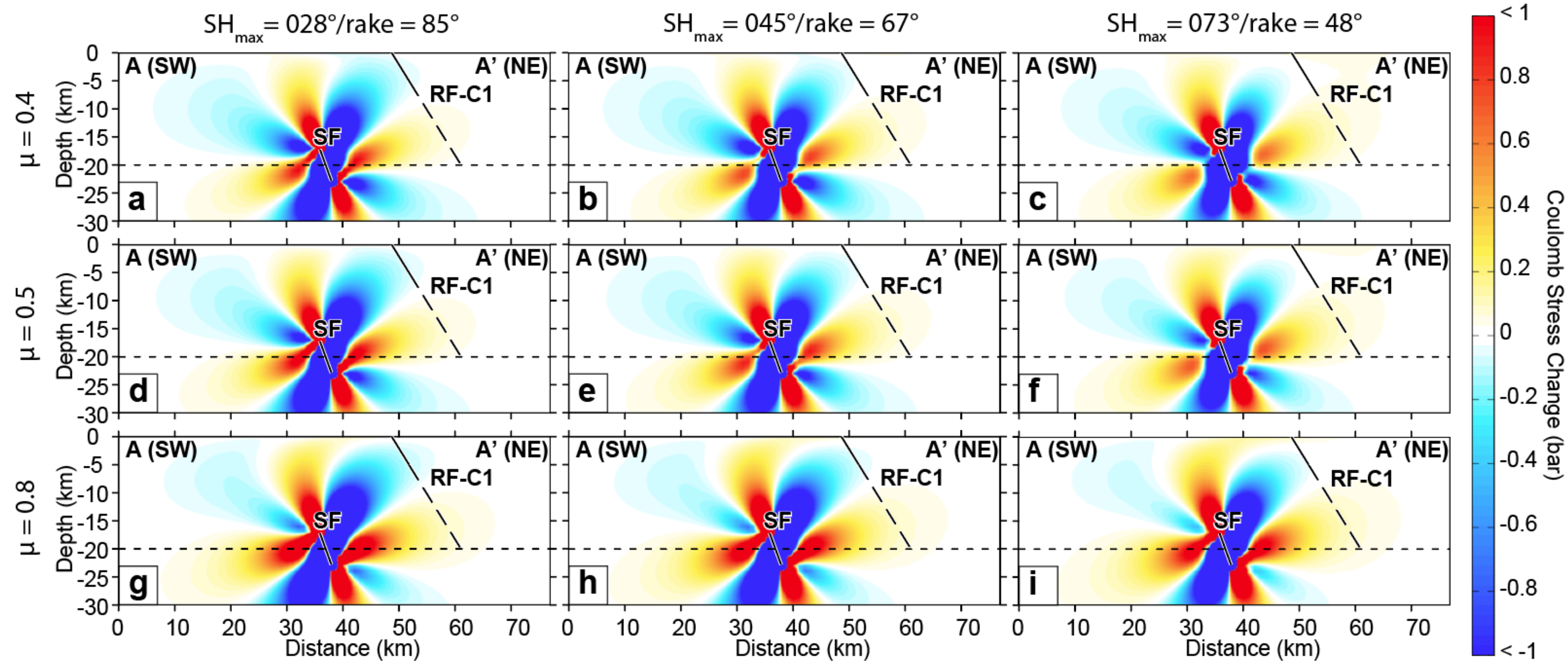

Figure S12. 1944 M_W 5.8 Cornwall-Massena Earthquake nodal plane 2 Coulomb stress change cross-sections. Coulomb stress changes for the NE-dipping source fault plane (strike = 313°, dip = 70°, rake = 52°), as seen in cross-sectional view. The sensitivity of stress change distributions was tested using the following receiver fault rake values (or maximum horizontal stress azimuths) as follows: (**a, d, g**) 85° (or S_{Hmax} = 028°), (**b, e, h**) 67° or SH_{max} = 045°, and (**c, f, i**) 48° (or SH_{max} = 073°); and coefficient of friction) values as follows: (**a, b, c**) μ = 0.4, (**b, e, h**) μ = 0.5, and (**c, f, i**) μ = 0.8.

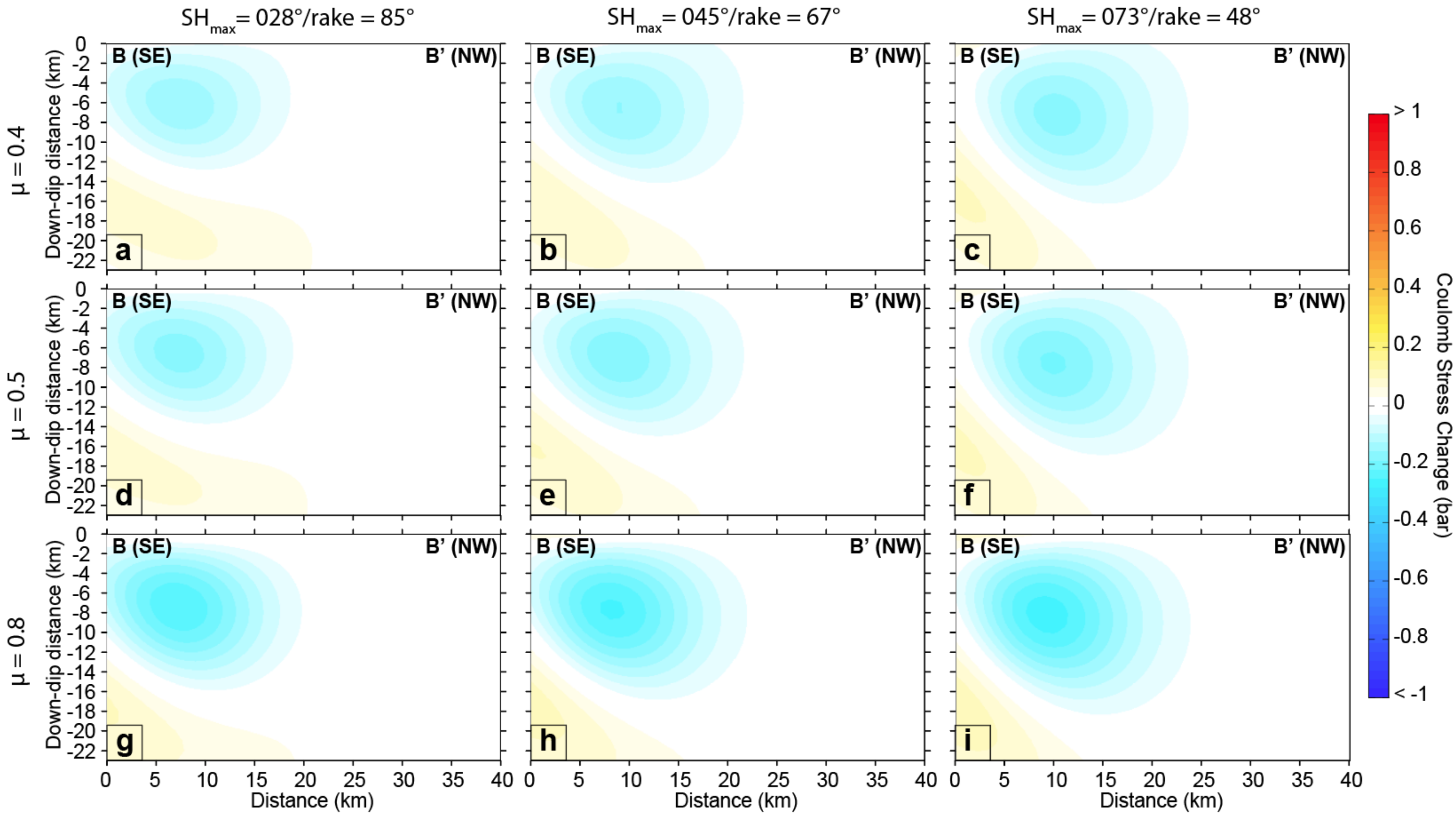

Figure S13. 1944 *M*$_W$ 5.8 Cornwall-Massena Earthquake nodal plane 1 Coulomb stress change on receiver faults. Coulomb stress changes for the NW-dipping source fault plane (strike = 199°, dip = 42°, rake = 149°), as seen on the receiver fault plane. The sensitivity of stress change distributions was tested using the following receiver fault rake values (or maximum horizontal stress azimuths) as follows: (**a, d, g**) 85° (or S_{Hmax} = 028°), (**b, e, h**) 67° (or SH_{max} = 045°), and (**c, f, i**) 48° (or SH_{max} = 073°); and coefficient of friction) values as follows: (**a, b, c**) μ = 0.4, (**b, e, h**) μ = 0.5, and (**c, f, i**) μ = 0.8.

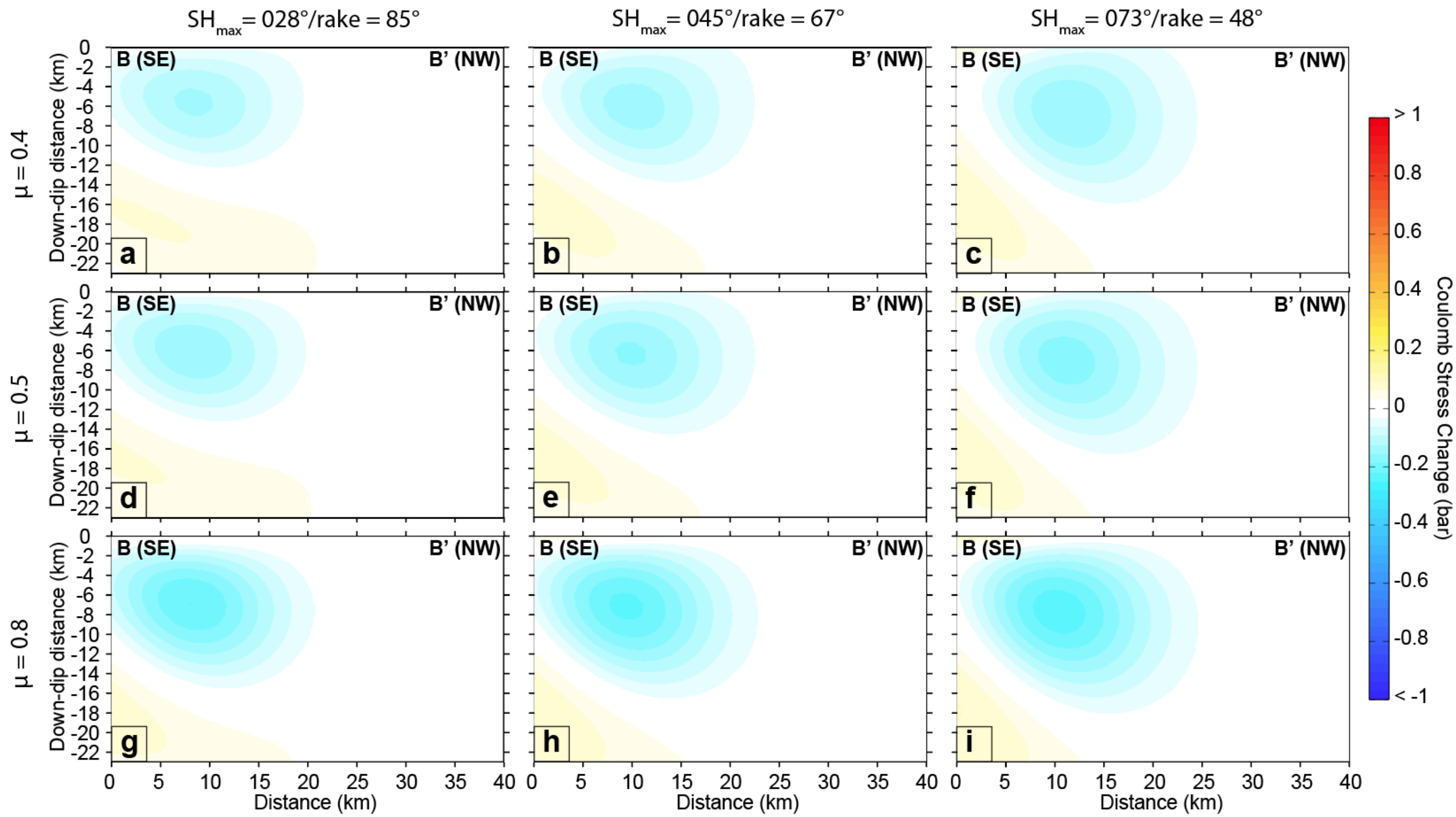

Figure S14. 1944 *M_W* 5.8 Cornwall-Massena Earthquake nodal plane 2 Coulomb Coulomb stress change on receiver faults. Coulomb stress changes for the NE-dipping source fault plane (strike = 313°, dip = 70°, rake = 52°), as seen on the receiver fault plane. The sensitivity of stress change distributions was tested using the following receiver fault rake values (or maximum horizontal stress azimuths) as follows: (**a, d, g**) 85° (or S_{Hmax} = 028°), (**b, e, h**) 67° or SH_{max} = 045°, and (**c, f, i**) 48° (or SH_{max} = 073°); and coefficient of friction) values as follows: (**a, b, c**) μ = 0.4, (**b, e, h**) μ = 0.5, and (**c, f, i**) μ = 0.8.

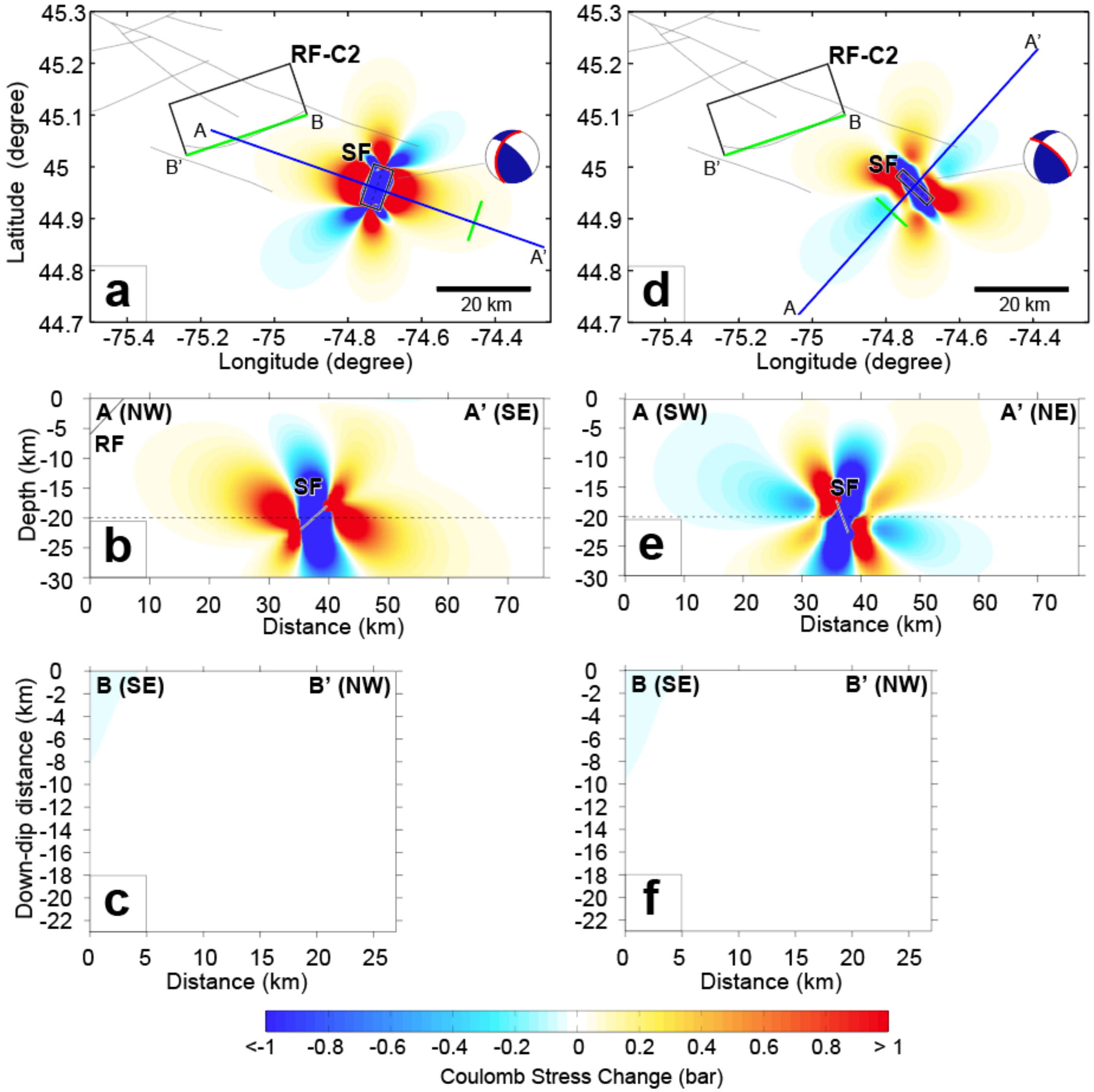

Figure S15. 1944 M_W 5.8 Cornwall-Massena Earthquake Coulomb stress changes for receiver fault 'RF-C2.' Map-view (20-km depth slice) (**a&d**), cross-sectional view (**b&e**), and receiver fault plane view (**c&f**) of the Coulomb stress changes for the NW-dipping (**a- c**) and NE-dipping (**d-f**) source fault planes (nodal planes 1 and 2, respectively; Table 1). All calculations assumed a coefficient of friction (μ) of 0.5 and a receiver fault plane rake of 67°, based on a maximum horizontal stress value (SH_{max}) of 45°.

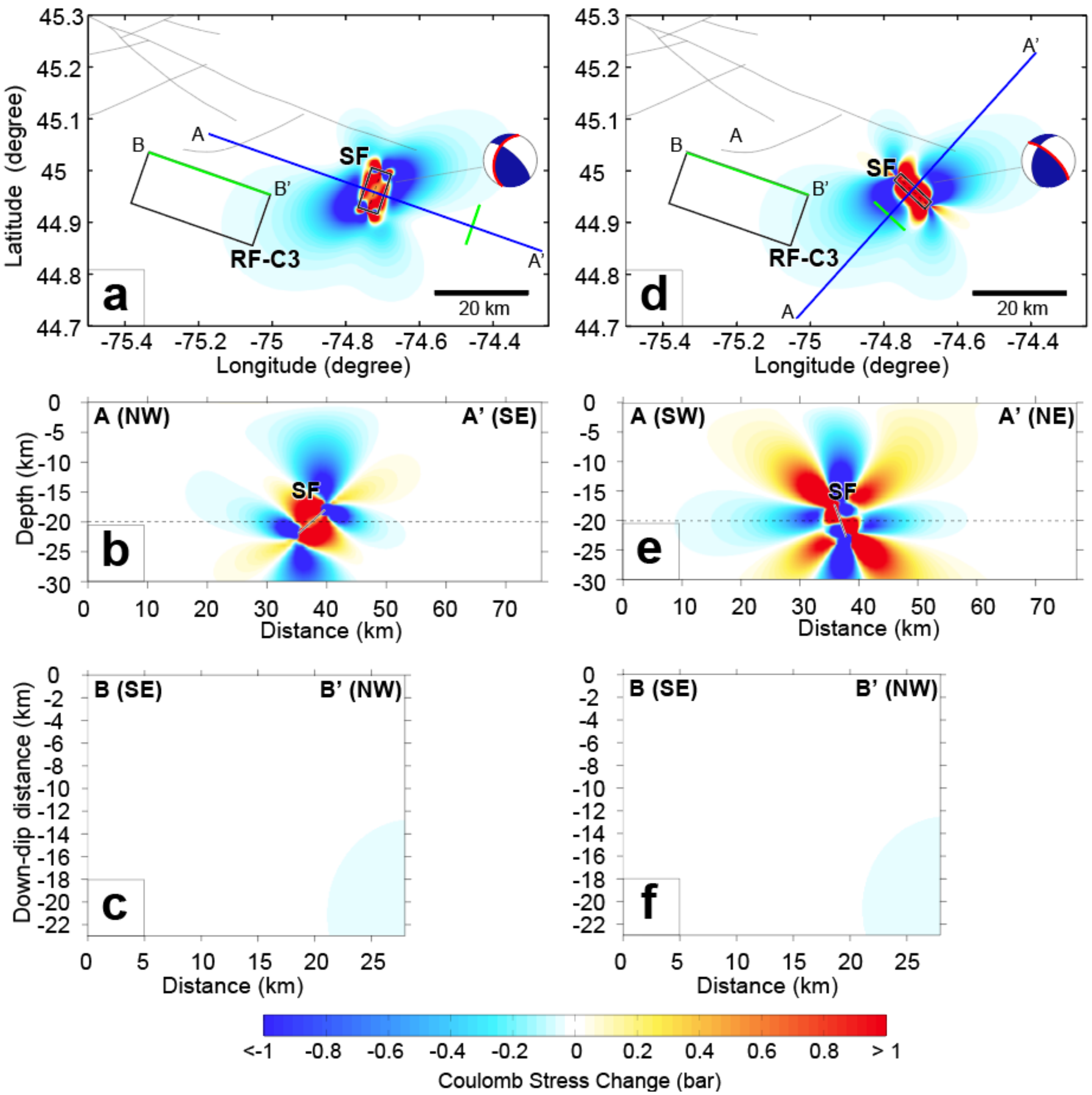

Figure S16. 1944 M_W 5.8 Cornwall-Massena Earthquake Coulomb stress changes for receiver fault 'RF-C3.' Map-view (20-km depth slice) (**a&d**), cross-sectional view (**b&e**), and receiver fault plane view (**c&f**) of the Coulomb stress changes for the NW-dipping (**a- c**) and NE-dipping (**d-f**) source fault planes (nodal planes 1 and 2, respectively; Table 1). All calculations assumed a coefficient of friction (μ) of 0.5 and a receiver fault plane rake of 67°, based on a maximum horizontal stress value (SH_{max}) of 45°.

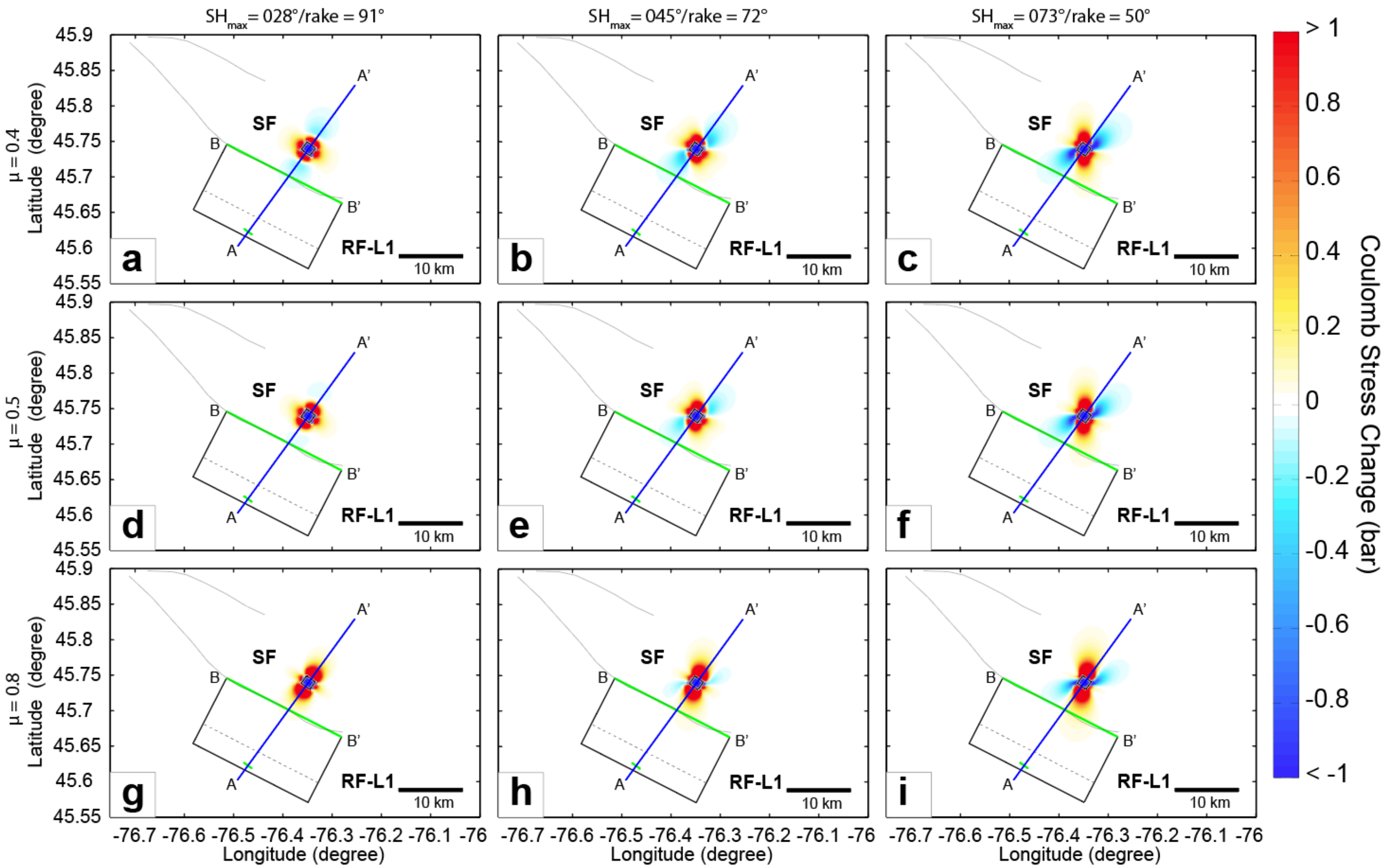

Figure S17. 2013 *M*$_W$ 4.7 Ladysmith Earthquake nodal plane 1 Coulomb stress change maps. Coulomb stress changes for the NE-dipping source fault plane (strike = 306°, dip = 41°, rake = 94°), as seen in map view (14-km-depth slice). The sensitivity of stress change distributions was tested using the following receiver fault rake values (or maximum horizontal stress azimuths) as follows: (**a, d, g**) 91° (or S_{Hmax} = 028°), (**b, e, h**) 72° (or SH_{max} = 045°), and (**c, f, i**) 50° (or SH_{max} = 073°); and coefficient of friction) values as follows: (**a, b, c**) μ = 0.4, (**b, e, h**) μ = 0.5, and (**c, f, i**) μ = 0.8.

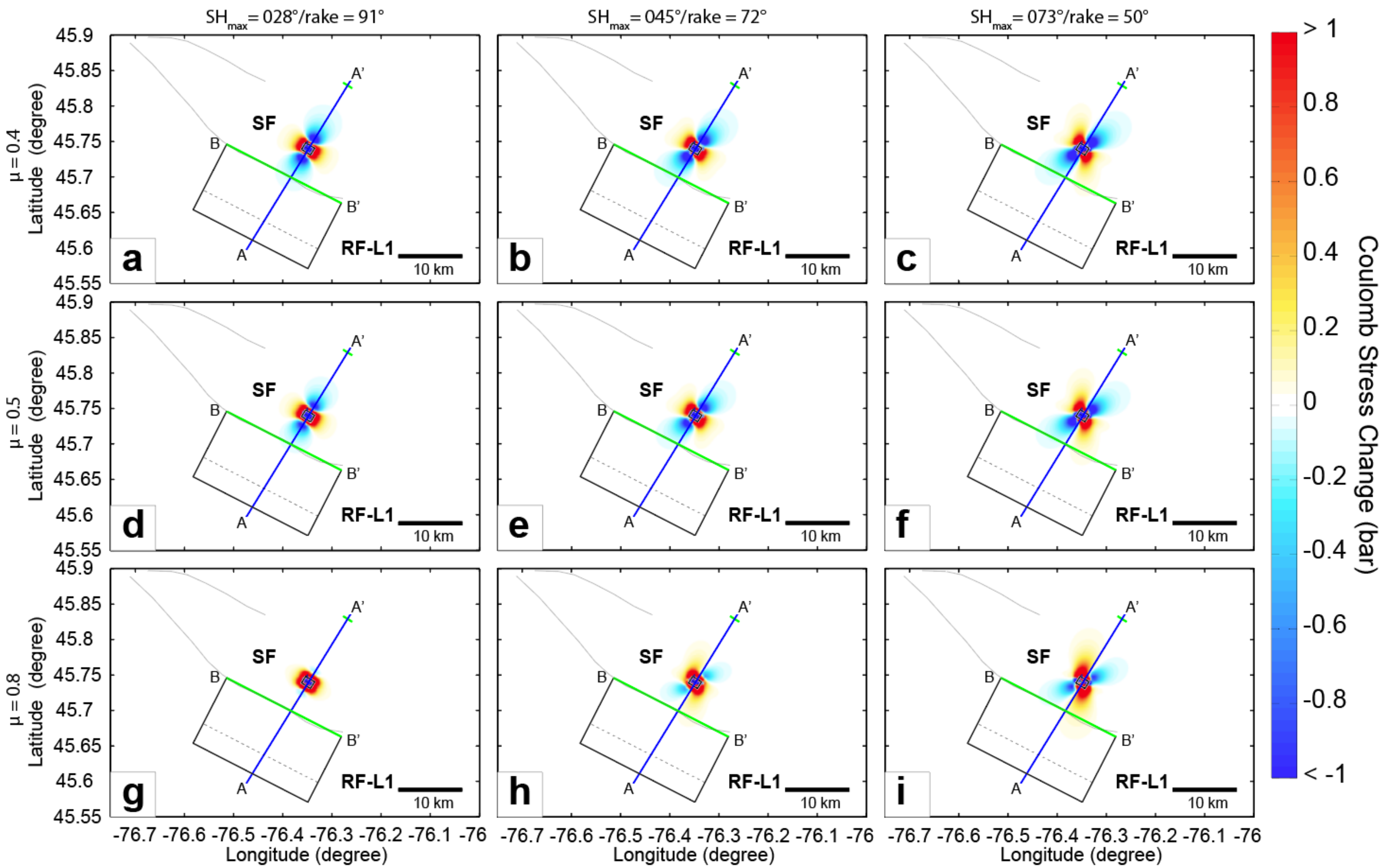

Figure S18. 2013 *Mw* 4.7 Ladysmith Earthquake nodal plane 2 Coulomb stress change maps. Coulomb stress changes for the SW-dipping source fault plane (strike = 122°, dip = 50°, rake = 87°), as seen in map view (14-km-depth slice). The sensitivity of stress change distributions was tested using the following receiver fault rake values (or maximum horizontal stress azimuths) as follows: (**a, d, g**) 91° (or S_{Hmax} = 028°), (**b, e, h**) 72° (or SH_{max} = 045°), and (**c, f, i**) 50° (or SH_{max} = 073°); and coefficient of friction) values as follows: (**a, b, c**) μ = 0.4, (**b, e, h**) μ = 0.5, and (**c, f, i**) μ = 0.8.

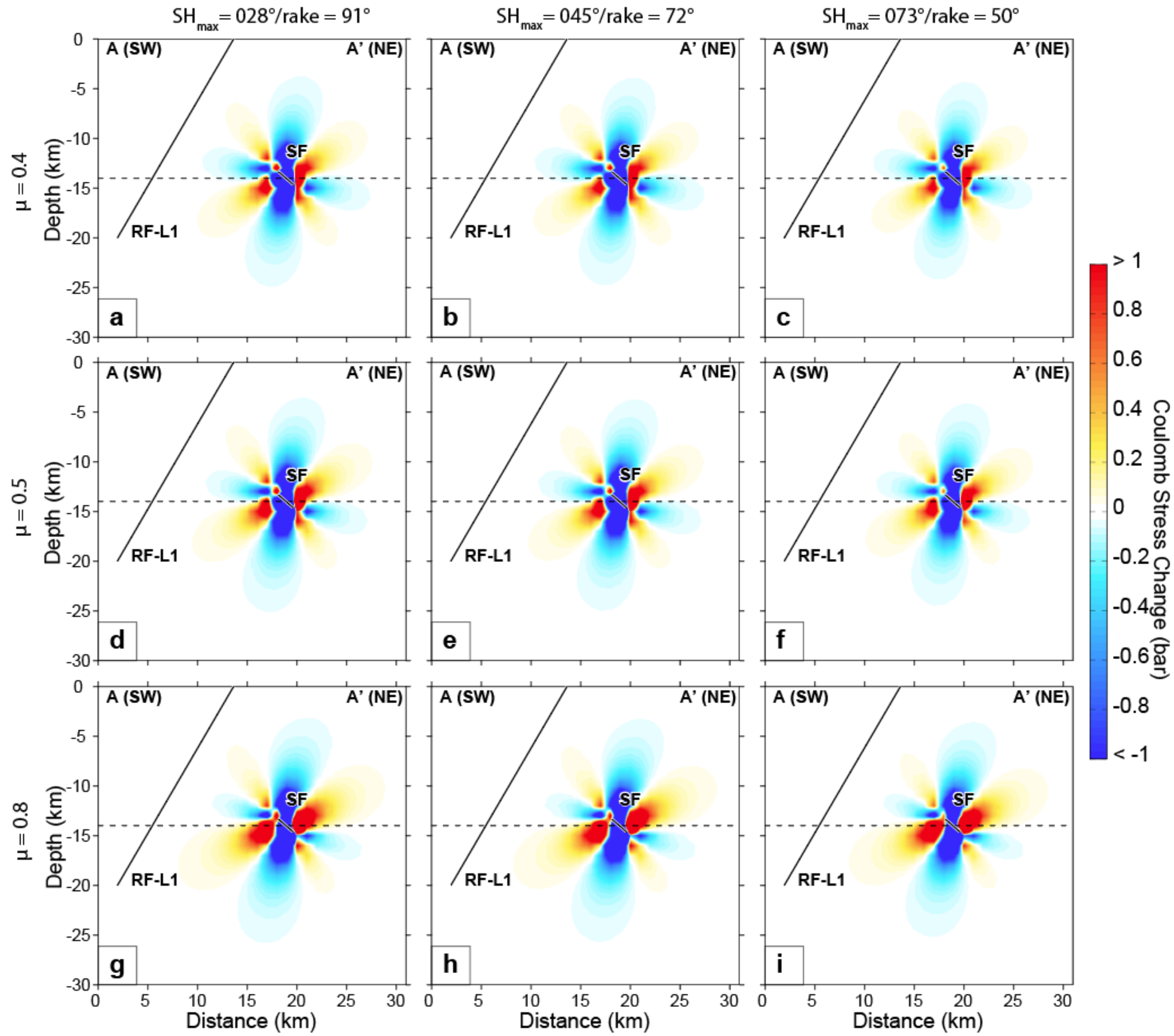

Figure S19. 2013 *Mw* 4.7 Ladysmith Earthquake nodal plane 1 Coulomb stress stress change cross-sections. Coulomb stress changes for the NE-dipping source fault plane (strike = 306°, dip = 41°, rake = 94°), as seen in cross-sectional view. The sensitivity of stress change distributions was tested using the following receiver fault rake values (or maximum horizontal stress azimuths) as follows: (**a, d, g**) 91° (or S_{Hmax} = 028°), (**b, e, h**) 72° (or SH_{max} = 045°), and (**c, f, i**) 50° (or SH_{max} = 073°); and coefficient of friction) values as follows: (**a, b, c**) μ = 0.4, (**b, e, h**) μ = 0.5, and (**c, f, i**) μ = 0.8.

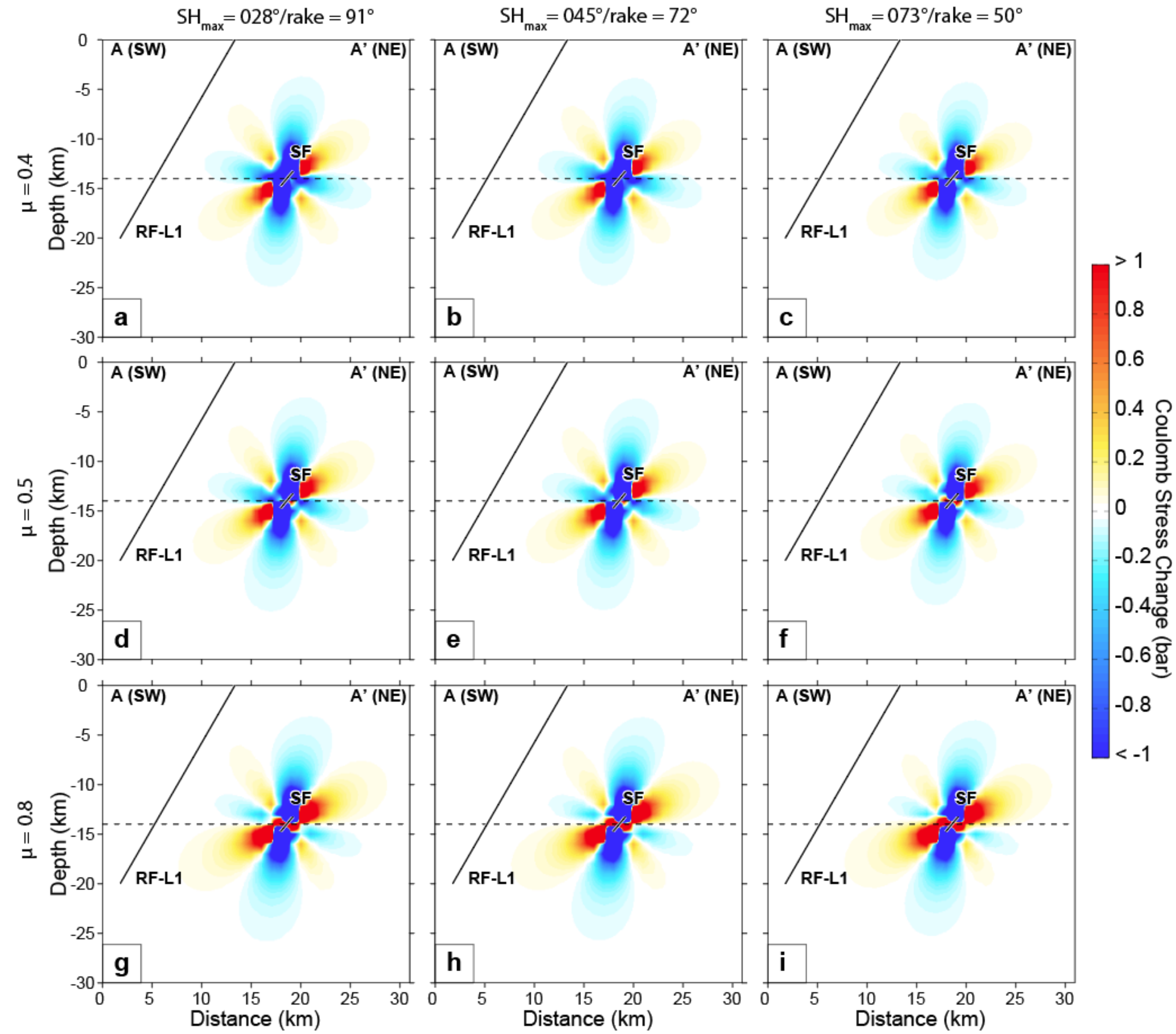

Figure S20. 2013 *Mw* 4.7 Ladysmith Earthquake nodal plane 2 Coulomb stress change cross-sections. Coulomb stress changes for the SW-dipping source fault plane (strike = 122°, dip = 50°, rake = 87°), as seen in cross-sectional view. The sensitivity of stress change distributions was tested using the following receiver fault rake values (or maximum horizontal stress azimuths) as follows: (**a, d, g**) 91° (or S_{Hmax} = 028°), (**b, e, h**) 72° (or SH_{max} = 045°), and (**c, f, i**) 50° (or SH_{max} = 073°); and coefficient of friction) values as follows: (**a, b, c**) μ = 0.4, (**b, e, h**) μ = 0.5, and (**c, f, i**) μ = 0.8.